AGU PUBLICATIONS

Geophysical Research Letters

RESEARCH LETTER
10.1002/2017GL074011

Key Points:
- Precipitation events are tracked in time and space over the whole globe for 1998–2014
- Relative to TRMM 3B42, ERA-Interim oversimulates average event duration and spatial footprint, and undersimulates average event intensity
- The number of 1–5 day events between 40 degrees S and 40 degrees N in the TRMM and ERA-Interim data has increased over the last two decades

Correspondence to:
R. H. White,
rachel.white@cantab.net

Citation:
White, R. H., D. S. Battisti, and G. Skok (2017), Tracking precipitation events in time and space in gridded observational data, *Geophys. Res. Lett.*, *44*, 8637–8646, doi:10.1002/2017GL074011.

Received 1 MAY 2017
Accepted 9 AUG 2017
Accepted article online 14 AUG 2017
Published online 26 AUG 2017

Tracking precipitation events in time and space in gridded observational data

R. H. White[1,2], D. S. Battisti[2], and G. Skok[3]

[1] JISAO, University of Washington, Seattle, Washington, USA, [2] Department of Atmospheric Sciences, University of Washington, Seattle, Washington, USA, [3] Faculty of Mathematics and Physics, University of Ljubljana, Ljubljana, Slovenia

Abstract Novel precipitation event data sets are created by tracking 3-hourly observed rainfall in both time and space in the TRMM 3B42 and ERA-Interim data sets. Relative to TRMM, ERA-Interim data undersimulate the total number of events (factor of ~0.5), and oversimulate the frequency of events lasting >5 days (factor of 1.6). Longer-lasting events tend to have larger spatial footprints and higher intensity precipitation at any point in their lifetime, and thus contribute significantly more to total precipitation than shorter events. Precipitation changes in selected tropical and subtropical regions are attributed to different event characteristics: some to changes in event rainfall intensity, others to changes in the number of events. In the 40°S–40°N spatial average, the number of events lasting 1–5 days significantly increased from 1998 to 2014 in both the TRMM 3B42 and ERA-Interim data. The event data sets, analysis scripts, and selected processed data are freely available online.

Plain Language Summary Personal experience tells us that rain occurs in individual events, yet when researchers study rainfall in observations and models we do not tend to focus on "event characteristics." Our work aims to change this, by presenting an analysis of event characteristics for all rain events that happened between 40°S and 40°N from 1980 to 2015. We look at how long events last (as they move through space), the average spatial footprint, or size, of events, and how much rain fell in total in an event. We set the stage for future work studying how "total event rainfall" may change in future climates, which may be crucial for estimating changes to the likelihood of flooding.

1. Introduction

The water cycle plays a vital role in Earth's climate and biosphere, and improving our understanding of variability in water availability is one of the current scientific Grand Challenges from the World Climate Research Programme [e.g., *Trenberth and Asrar*, 2014]. In a warmer climate, the hydrological cycle is expected to intensify [e.g., *Held and Soden*, 2006; *Bates et al.*, 2008; *Allan et al.*, 2010]. The manifestation of such an intensification at local levels, however, remains uncertain [*Collins et al.*, 2013].

Looking at climatological time mean precipitation provides a useful metric for studying precipitation changes; however, personal experience tells us that precipitation occurs in discrete events. *Venugopal and Wallace* [2016] estimate that at any given instant half of all tropical rain is concentrated within only ≈1% of the tropics. At one end of the spectrum are small, highly localized events, such as those associated with tropical convective cells, while at the other end lie long-lasting events with large spatial footprints, such as in tropical or extratropical cyclones.

Almost 15 years ago, *Trenberth et al.* [2003] highlighted the need for more research on precipitation intensity, frequency, and duration of events, in both observations and models. They note that while the intensity of precipitation falling in individual storms may increase in a warmer climate, understanding storm duration changes is key to fully discerning how total event precipitation may change. In addition, studying the spatial footprint of precipitation events is important for understanding flooding risks: intense precipitation over a whole river basin is more likely to result in downstream flooding than equally intense precipitation over a fraction of the basin.

The distribution of precipitation in mesoscale convective systems and in the diurnal cycle of precipitation has been well documented [e.g., *Nesbitt et al.*, 2000; *Nesbitt and Zipser*, 2003; *Houze et al.*, 2015]. Some of this work

was extended to include identification of discrete cloud features [*Liu et al.*, 2008], and the identification of atmospheric fronts and associated precipitation [*Berry et al.*, 2011; *Catto et al.*, 2012] using objective detection algorithms. The aforementioned studies examine snapshots of precipitation in time, without connecting features from consecutive time periods into precipitation "events." Using 3-hourly precipitation observations, *Liu* [2010] classified long-duration precipitation events as times when an event produced rainfall in a grid cell for four consecutive 3-hourly periods.

One of the first algorithms to track precipitation features in both space and time was developed by *Davis et al.* [2006] and used to study mesoscale rain events over the U.S. and evaluate the forecast ability of a regional climate model. *Skok et al.* [2010] modified this event identification technique to evaluate modeled precipitation event characteristics over the Pacific Ocean. A similar technique was used by *Chang et al.* [2016] to study rainfall events over the U.S., including future changes simulated by a regional climate model with a "business-as-usual" emissions scenario. These studies find that relative to observations, models tend to produce events that are longer lived and have larger spatial footprints and lower rain intensities.

In this study we present results from two new data sets, created by tracking precipitation events in both time and space in the Tropical Rainfall Measuring Mission (TRMM) 3B42 and ERA-Interim observational data sets, using the method developed by *Skok et al.* [2009]. We look at event characteristics of average spatial footprint, total precipitation, and rain intensity, as a function of event duration. We emphasize that in this study, when we refer to event duration we do not mean how long it rained in one particular location, but the lifetime of the event when tracked in both space and time. To the authors' knowledge, the data sets we present in this study are the first such data sets of precipitation events across all longitudes. The data sets and all analysis code have been made freely available online (see Acknowledgments section for URL).

2. Event Database Creation

2.1. Tracking Algorithm

To identify and track discrete precipitation events, we use the "forward-in-time" (FiT) algorithm developed by Gregor Skok with collaboration from researchers from the National Center for Atmospheric Research. Full details can be found in *Skok et al.* [2009, 2010, 2013]; here we present a brief overview. The first step is to define thresholds in the precipitation rate that delineate events. The use of multiple thresholds allows the algorithm to distinguish distinct but neighboring meteorological systems. At all time steps, the algorithm identifies all unique objects within the thresholded data. The FiT algorithm then finds objects that are linked across multiple time steps: if any part of the object at time t overlaps spatially with any part of an object at time $t+1$, these objects are considered a single event. The forward-in-time aspect allows an event to split into multiple objects and retain a single identity, but does not allow two objects that are initially unique to merge at any later time step. The FiT algorithm code is a freely available software package (obtainable from author Gregor.Skok@fmf.uni-lj.si).

Identifying and tracking all events in 16 years of 3-hourly $0.25° \times 0.25°$ TRMM 3B42 data takes only 48 h using a single node of a 32 core, x86_64 linux system, as the algorithm is highly optimized for speed. The postprocessing code in python takes advantage of array computations to process the 65,700,428 events and runs in under 4 days on the same system.

2.2. Precipitation Data Sets

The tracking algorithm described above requires gridded precipitation at high temporal resolution in order to correctly identify fast-moving events as a single event, and high spatial resolution to distinctly identify events with small spatial footprints. The 3-hourly, $0.25° \times 0.25°$, TRMM 3B42 (V7) gridded observational data set is the highest resolution data set available for the study of events across all longitudes. This data set is one of the TRMM Multisatellite Precipitation Analysis (TMPA) products produced as part of the Tropical Rainfall Measuring Mission (TRMM) [*Simpson et al.*, 1996; *Adler et al.*, 2000] Multisatellite Precipitation Analysis (TMPA) by the NASA Goddard Space Flight Center [*Huffman et al.*, 2007; *Huffman and Bolvin*, 2014]. To construct the TRMM 3B42 data set, the TRMM's precipitation radar (PR) product calibrates infrared and microwave precipitation estimates from various satellites, with adjustment by monthly analyses from ground-based precipitation measurements [*Huffman et al.*, 2007]. The merging of data sets produces an unprecedented view of the spatial and temporal evolution of precipitation in the tropics and subtropics, opening a gateway to the characterization and study of tropical precipitation in a manner that was not previously possible [e.g., *Kikuchi and Wang*, 2008; *Venugopal and Wallace*, 2016].

The blending of data sets is necessary to produce a global-scale data set with both high temporal and spatial resolution; however, such a method is not without caveats. The main disadvantage is the lack of consistency in time; the input products change as old satellites are retired, new satellites are launched, and satellite orbits are adjusted [*Huffman et al.*, 2007; *Huffman and Bolvin*, 2014]. Since the beginning of the TRMM in 1998, there has been an ongoing increase in the number of microwave sounding units available for inclusion into the blended product. Much work has been done to blend all the data as seamlessly as possible [*Huffman and Bolvin*, 2014]; however, some seams undoubtably remain, and thus this product is not considered a climate data record.

For the analysis presented here, we choose thresholds equal to those given by *Skok et al.* [2013]: 24, 40, 56, 80, and 120 mm d^{-1} (i.e., 3, 5, 7, 10, and 15 mm in 3 h). The analysis was repeated with higher thresholds (lowest threshold 48 mm d^{-1}) and with an additional lower threshold of 6 mm d^{-1}. The conclusions presented in this paper are insensitive to these threshold changes. Imposing a smaller minimum threshold increases the number of identified events and includes more of the total precipitation in the analysis; however, using too low a threshold leads to unrealistically large-scale events as the finite spatial resolution connects nearby drizzling pixels into one superevent. By excluding very light rain from the analysis, we aim to remove biases related to changes in the detection of light rain by some of the satellite instruments in the TRMM 3B42 data set [*Huffman et al.*, 2007; *Berg et al.*, 2009].

In the merged TRMM 3B42 data set there are very few missing data points. Prior to running the FiT analysis code; however, we remove any missing values in the following manner: if there is a nonmissing value at the grid point in question for the time step before and after the missing value, then the missing value is set to the temporal average; otherwise, the missing value is set to 0. The results in this paper are insensitive to how the missing data are treated.

The smallest and shortest duration-detectable "event" is limited by the resolution of the observational data set: 0.25°× 0.25° with 3-hourly time resolution. Additional limitations exist as we assume precipitation falling continuously throughout each 3-hourly period; in reality the TRMM data are instantaneous snapshots of precipitation rates. If multiple sub-3-hourly events occur in consecutive 3-hourly periods, the algorithm will misclassify these as a single longer-lasting event. An additional issue with the time resolution is that well-organized, narrow (one grid box wide), events that move more than two grid boxes per time step (approximately 4 m/s), may not always be contiguous in space from one time step to the next; events such as narrow squall lines may therefore be erroneously identified as multiple short-lived events. Additionally, the TRMM data set smooths out any subgrid-scale variations in precipitation. The algorithm will miss events with small subgrid-scale spatial footprints unless they have a high enough rain rate that the average over the grid box exceeds the minimum threshold of 24 mm/d. The algorithm will also erroneously consider multiple subgrid-scale events to be a single event. We explore some of the effects of spatial resolution when we regrid the TRMM 3B42 data onto the larger ERA-Interim grid and by repeating our analysis with the smallest events excluded.

We conduct a comparison of the climatology of events in the TRMM 3B42 data set with that from the 3-hourly ERA-Interim reanalysis data [*Dee et al.*, 2011]. We obtain the ERA-Interim data on a regular latitude-longitude grid with resolution 0.75° × 0.75°; the data were regridded from the native spectral T255 grid by the ECMWF's Meteorological Archive and Retrieval System. We extract 3-hourly precipitation from the 3, 6, 9, and 12 h forecasts of accumulated precipitation. As resolution can strongly affect the detection of precipitation events, for this comparison analysis we run the event tracking software on the TRMM and ERA-Interim data on the same grid; we regrid the higher-resolution TRMM data to the ERA-Interim 0.75° × 0.75° grid using the Earth System Modeling Framework (ESMF) conservative regridding routine within the NCAR Command Language. While precipitation in the ERA-Interim data is produced directly by the model, the model assimilates rain-affected satellite measurements [*Bauer et al.*, 2006], including some measurements used in the merged TRMM 3B42 data set; these data sets are therefore not completely independent.

3. Results

We explore the climatology of precipitation events around the globe, including separating events by duration, before moving on to investigate decadal-scale changes. The benefit of tracking objects in both space and time is that it allows the study of temporal aspects of precipitation events such as total duration, event mean rainfall intensity, and propagation speed.

Table 1. Average Characteristics of Events of Different Durations, for 40°S to 40°N

Duration	Events/yr (%)	Precipitation, mm/d (%)[a]	Footprint ($\times 10^4$ km^2)[b]	Intensity (mm/d)
TRMM	3.3×10^6	2.5	0.33	47
0–1 day	99.4%	57%	0.31 (4.3)	47
1–2 days	0.6%	25%	3.8	79
2–5 days	0.07%	13%	7.5	88
>5 days	0.003%	3.4%	14.7	99
TRMM ERAI grid	5.1×10^5	2.1	1.8	43
0–1 day	98.0%	48%	1.6 (2.5)	43
1–2 days	1.7%	28%	8.9	70
2–5 days	0.3%	18%	15.0	73
>5 days	0.02%	6.3%	23.3	80
ERAI	2.2×10^5	0.86	2.1	27
0–1 day	97.7%	30%	1.8 (2.7)	27
1–2 days	1.6%	18%	10.3	39
2–5 days	0.6%	30%	18.5	43
>5 days	0.09%	21%	35.6	44

[a]Precipitation in mm/d is the domain average precipitation associated with all events and the fraction of this precipitation as a function of event duration. For reference, total domain average precipitation for TRMM (ERA-Interim) for this time period is 3.0 mm/d (3.3 mm/d).

[b]Event footprint is the average 3-hourly spatial footprint over the duration of the event. For 0–1 day events the equivalent value in grid boxes is shown in parentheses for comparison, based on the average grid box size in the whole analysis region.

3.1. Climatology

Characteristics for events between 40°S and 40°N are shown in Table 1 for all events (first line for each data set) and then as a function of event duration. These values take into account changes in grid box size with latitude. We remove the most northern and southern 10° of the TRMM 3B42 data (40–50°N/S) to avoid a low bias in the lifetime and footprint of events in this region due to events leaving or entering the TRMM domain. Events lasting less than 1 day dominate in number, consistent with the log-log relationship between number of events and duration shown by *Skok et al.* [2010]. Despite accounting for less than 1% of precipitation events, 25% of all rain falls in 1–2 day events: 1–2 day events last longer than 1 day events by definition, and events with longer durations tend to be larger (footprint column) and have more intense rainfall at any given time (intensity column).

To illuminate some of the impacts of resolution on our results, we rerun our analyses considering only events that span at least four unique grid boxes over their lifetime (unique defined in space, such that an event is not included if it only occupies the same single grid box for four time steps). The total number of events identified drops by 2/3, to 1.2×10^6, and average footprint (intensity) for 0–1 day events increases from 0.31 to 0.66×10^4 km^2 (47 to 57 mm d^{-1}). Other changes are small: the percentage of 0–1 day events decreases from 99.4% to 98.3%, while the fraction of total precipitation captured by all events drops from 81% to 78%. Our results are therefore largely insensitive to the issues regarding the smallest events, e.g., subgrid-scale convective elements.

Figure 1a shows the spatial distribution of average event density in events per grid box per year, showing the average number of events each grid box sees passing through each year. Each event is counted only once in each grid box it travels over—this field therefore provides a different metric to "rain frequency" counts of how many 3-hourly periods in a year had precipitation above the minimum threshold. Events with large spatial footprints will be counted in many grid boxes. On average, ocean points see 60.3 events/yr, while land points see 58.4 events/yr. With an average event lifetime of 4.1 h, this gives an estimated average total rain time of 246 h per year, equivalent to an average rain frequency of 3%, consistent with *Yang and Nesbitt* [2014].

Figure 1b shows the percentage of total precipitation captured in events at each point. Running the algorithm with the standard precipitation thresholds (see section 2.2), 81% of total precipitation in this domain is identified as part of an "event"; the remaining 19% therefore falls at less than our minimum threshold of 24 mm d^{-1}.

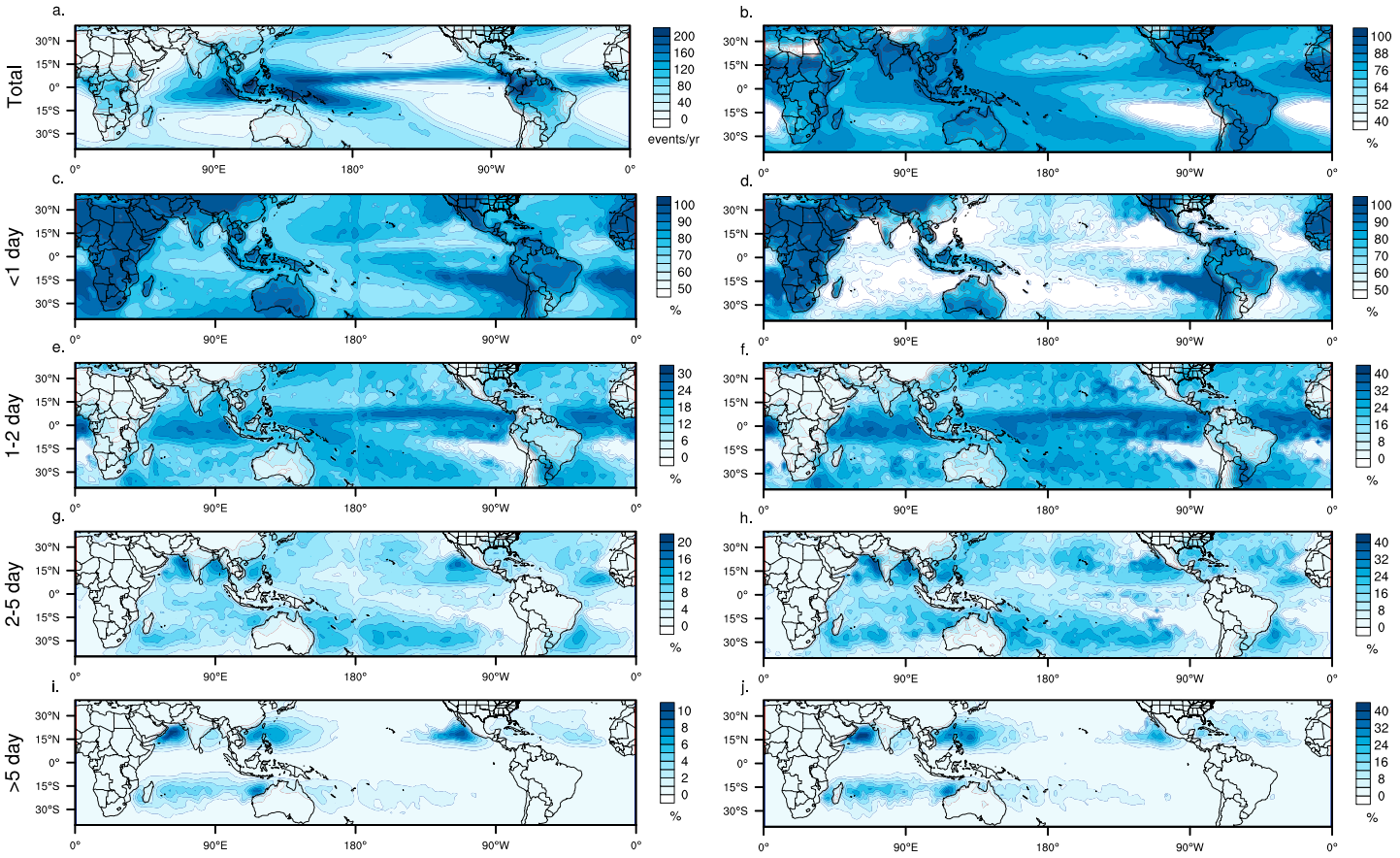

Figure 1. Event statistics in the TRMM 3B42 data set, separated by event duration. (a, c, e, g, and i) Percentage of all events at each grid box in duration range. (b, d, f, h, and j) Percentage of total annual event precipitation falling in events in each duration range. Data have been conservatively regridded onto a grid approximately 2° × 2°.

In the remainder of this paper "total precipitation" refers to the total TRMM 3B42 precipitation, while "event precipitation" is that identified as part of an event (i.e., falling at >24 mm d^{-1}).

The remaining panels on the left side of Figure 1 show the spatial distribution of events as a function of event duration, given as a percentage of total events seen by each grid box (note changes in color scale for each plot). While events lasting >5 days account for 0.003% of all events (see Table 1), they often occur in regions experiencing very few rain events overall, and thus account for >10% of all events seen by some regions. The increase of shorter duration events along 180°E (and decrease in longer events) is an artifact of the tracking code not connecting −180°E to 180°E (the current version of FiT does not support periodic domains).

The percentage of event precipitation falling as a function of event duration is shown in the right column of Figure 1. Longer-lasting events contribute more to precipitation than they do to event density: for example, in the northwest Indian Ocean 40% of event precipitation falls in events lasting >5 days, despite such events accounting for only ∼10% of events seen by these regions. This is consistent with the data in Table 1: longer events tend to have more intense rainfall and larger spatial footprints (thus, they are more likely to rain in one place for longer).

Stephens et al. [2016] found that precipitation happens more frequently in the Southern Hemisphere, but more intensely in the NH. Our data set can provide an event-based analysis of this, albeit only for the region 40°S–40°N. For all event duration categories the Northern Hemisphere has more precipitation events that are on average about 3% smaller (2–5 day events around 10% smaller), and on average 1–3% more intense.

3.2. ERA-Interim Comparison

Here we present a preliminary comparison of precipitation events from the TRMM data set with those in ERA-Interim. For the ERA-Interim data we perform event tracking for the whole globe; however, here we focus

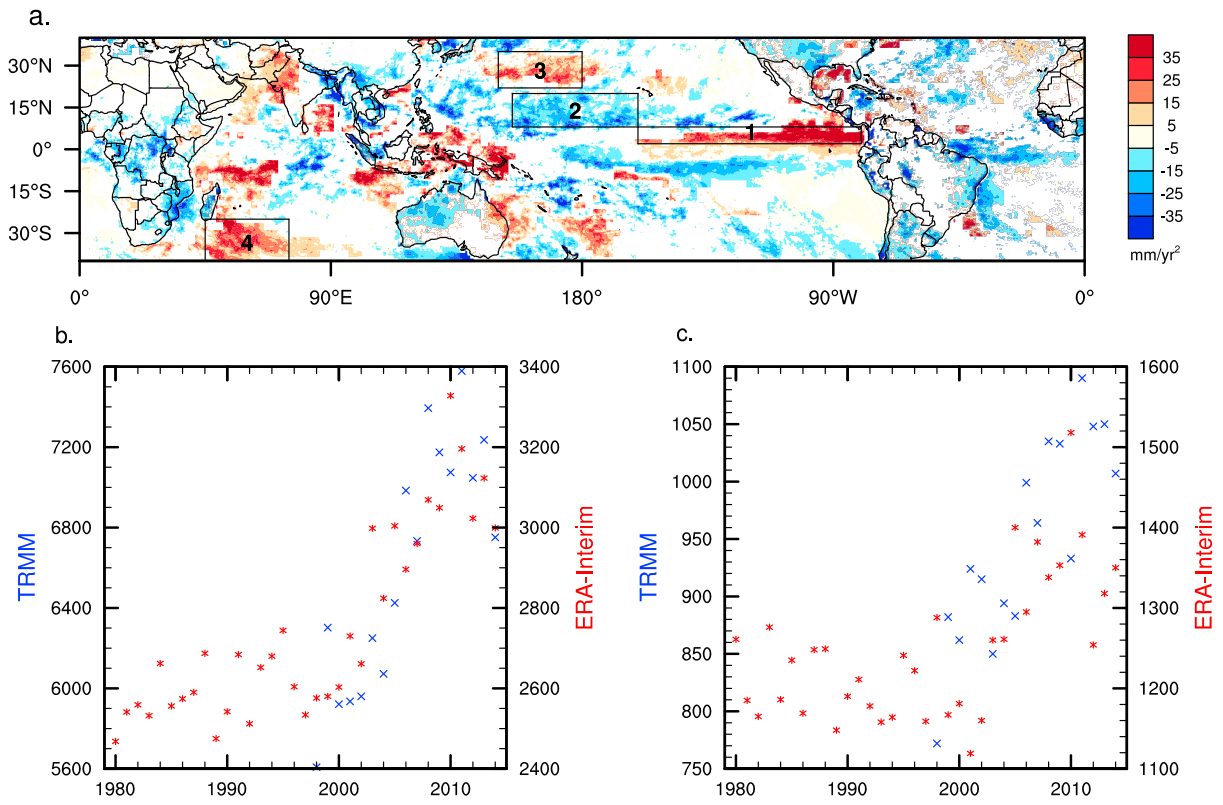

Figure 2. (a) Linear regression in time of annual precipitation from TRMM 3B42 data set from 1999 to 2014. Data whited out where the sign of the regression is inconsistent with the sign of regressed NOAA outgoing longwave radiation data. (b) Annual number of 1–2 day events in the TRMM data set (blue crosses) and ERA-Interim (red stars). (c) As in Figure 2b but for the number of 2–5 day events.

on the region from 40°S to 40°N for comparison with the TRMM 3B42 data. Results are summarized in Table 1. Regridding the TRMM data to the ERA-Interim lower spatial resolution (TRMM ERAI grid in Table 1) reduces the number of events detected by 85%. Using the same thresholds as before, 73% of the regridded TRMM precipitation is identified as part of an event, compared to 26% of all precipitation in ERA-Interim; thus, the amount of precipitation falling at >24 mm d^{-1} is substantially underestimated by ERA-Interim relative to the TRMM data set.

Despite having fewer than half the number of events than the regridded TRMM data, ERA-Interim produces approximately 1.6 times as many events lasting >5 days. Consistent with this, ERA-Interim underestimates the fraction of precipitation from events lasting <2 days while overestimating that from long-lasting events: converting values in Table 1 to total precipitation, 6.0% versus 3.9% of the total precipitation falls in events >5 days for ERA-Interim and TRMM, respectively. The ERA-Interim data set also overestimates the average spatial footprint and underestimates the average intensity, particularly for longer-lasting events.

3.3. Local Decadal Variability

Using case studies of localized regions, we demonstrate how this event-tracking method can be used to study changes in precipitation characteristics. The regions are chosen based on large linear trends in precipitation from 1999–2014 (avoiding the anomalously large El Niño in 1997–1998). The spatial pattern of linear regressions between 1999 and 2014 is shown in Figure 2, with the chosen regions outlined in black; grid boxes are masked to white where the sign of the linear trend is inconsistent with the linear trend in NOAA Interpolated Outgoing Longwave Radiation (OLR) [*Liebmann and Smith*, 1996] data set (assuming OLR and precipitation should be inversely correlated). As these data sets are independent, this increases our confidence that we are studying real variability in precipitation, rather than changes related to the evolution of the satellites and observing systems in the TRMM data set. The spatial pattern shows similarities to that found by *Gu et al.* [2016] in the Global Precipitation Climatology Project (GPCP) data set between 1979 and 2012.

Table 2. Linear Regressions (1999–2014) of Event Precipitation in Each Region, Followed by Regressions in Precipitation Characteristics for Events of Different Durations[a]

Region	Total Precipitation Trend (mm/yr^2)	Event Duration	Precipitation (mm/yr^2)	Number (events/yr)	Intensity (mm/event/yr)
1	22 (1.5%)	<1 day	14 (2%/yr)*	–	0.001 (1%/yr)*
2	−3 (0.4%)	>5 days	−2.5 (−1%/yr)	−0.15 (−14%/yr)*	–
3	14 (1.5%)	1–2 days	5.2 (2%/yr)*	5.5 (3%/yr)*	−0.5 (−3%/yr)*
		2–5 days	4.7 (4%/yr)*	0.7 (3%/yr)	1.6 (3%/yr)
4	18 (2.7%)	<1 day	7.4 (2%/yr)*	–	0.003 (2%/yr)*
		1–2 days	7.1 (5%/yr)*	5.9 (5.%/yr)*	–
		2–5 days	2.7(3%/yr)	0.8 (3%/yr)*	–

[a]Different durations are color coded as well as noted in the table: <1 day; 1–2 days; 2–5 days, and >5 days. Only values that are statistically significant at $p < 0.1$ are shown.
*Significant at $p < 0.05$.

The selected regions are analyzed to determine how precipitation trends are manifest as changes in event number and intensity as a function of event duration; results are summarized in Table 2. Linear regression coefficients are shown for event precipitation; these values are similar to those for total precipitation, except for region 2, where much of the decrease is in precipitation falling at less than the minimum threshold of 24 mm d^{-1}, and thus event precipitation shows smaller regressions.

Regions 1, 3, and 4 show increases in precipitation over this period, while region 2 shows a decrease; all regressions are statistically significant at the $p < 0.1$ level for a two-sided p value as calculated by a Wald Test with a t distribution test statistic (from scipy.linregress). We emphasize that these regions are chosen specifically because they feature large trends in precipitation over the time period studied, and should not be considered suggestive of long-term or global changes in precipitation.

In region 1, in the eastern Pacific deep tropics, the increase in precipitation is due to an increase in the amount of precipitation falling in events lasting <1 day. The decrease in precipitation in region 2 is primarily due to a decrease of rain falling below the minimum threshold of 24 mm d^{-1}; however, there is also a negative trend in the number of events lasting >5 days. In regions 3 and 4, farther away from the tropics, increases in precipitation are due to increases in the number of events lasting 1–2 and 2–5 days and an increase in the average intensity of rain during events lasting <1 day.

The increase in the number of 1–2 and 2–5 day events over regions 3 and 4 is suggestive of an increase in storminess. Consistent with this, we find significant increases in annual-mean 200 mb eddy-kinetic-energy (EKE) calculated from ERA-Interim data, when averaged over region 3 or 4 (EKE was calculated as the time mean of 6-hourly values of $0.5(u'^2 + v'^2)$, where $'$ denotes the anomaly from the zonal mean).

There is a significant increase in the number of events lasting 1–2 days in each of regions 1, 3, and 4; in regions 1 and 3 this increase is ameliorated by a decrease in the amount of precipitation per event, to the extent that in region 1 there is no significant trend in precipitation from these events. Consistent with these increases, highly significant trends are found for the whole region of 40°S–40°N in the number of 1–2 day events (1.6%/yr) and 2–5 day events (1.9%/yr). For both duration bands, there is a related significant increase in precipitation from these events, despite decreases in the corresponding event intensity.

The time evolution of the annual number of 1–2 and 2–5 day events between 40°S and 40°N is shown for the TRMM and ERA-Interim data sets in Figures 2b and 2c. The ERA-Interim data provide a first check on whether this strong "trend" is an artifact of the observing system. While the TRMM and ERA-Interim data are based on some of the same satellite data, Figures 2b and 2c show that the interannual variability of the number of events is not closely correlated between the two data sets; only the long-term trend is similar. The ERA-Interim data show a weak, but statistically significant ($p < 0.05$) increase in the number of 1–2 day events between 1980 and 2003; since around 2003 the trend has been much stronger. The strength of the recent trend is unlikely to be influenced by the anomalous positive shift in ERA-Interim precipitation in 2006 associated with changes in the number of assimilated observations of total column water vapor [*Dee et al.*, 2011], as the strongest increase in 1–2 day events occurs prior to 2006 (Figure 2b).

4. Discussion

We present a climatology of precipitation events tracked in space and time for 40°S–40°N from 1998 to 2014. To the authors' knowledge, this is the first data set to study the characteristics of precipitation in a way that is not restricted to a local region.

Shorter events have, on average, lower intensity rainfall and smaller spatial footprints, and although events lasting <1 day make up over 99.3% of all identified events, they make up only 57% of total event precipitation. If we make the approximation that much of the precipitation falling in events lasting less than 1 day is associated with convection, then this result is consistent with the work of *Yang and Nesbitt* [2014], who suggest that 52% of precipitation from the TRMM precipitation radar can be categorized as convective precipitation.

This method could become a useful tool to characterize and compare precipitation events simulated by high-resolution general circulation models with observed events. Understanding how biases manifest in terms of event durations, intensity, travel speeds, and spatial sizes may help guide attempts to improve convective parameterization schemes and ultimately reduce model precipitation biases. We demonstrate such a comparison on the ERA-Interim reanalysis data set, finding that much more precipitation falls at <24 mm d^{-1} in the ERA-Interim data (74%) relative to regridded TRMM data (27%). Some of this difference is due to an underdetection of light rain by the TRMM data product [*Huffman et al.*, 2007]; however, *Berg et al.* [2009] estimate that the TRMM precipitation radar misses about 10% of total rain, and thus this is not the sole, or even dominant, cause. This overestimation of the frequency of light rain is consistent with findings from general circulation models [e.g., *Dai*, 2006]. This bias in rainfall rate contributes to half as many events being detected in ERA-Interim relative to TRMM. Of the events that are detected, the ERA-Interim data set is biased toward producing too many long-lived events, that are too large, but have too low intensities.

As an analog for studying the changing character of precipitation events in climate model projections, we perform an analysis of localized trends in the TRMM data set. We choose four regions that have shown significant changes in precipitation over the TRMM time period. In the eastern tropical Pacific region, the increase in precipitation is caused predominantly by an increase in precipitation per event for events lasting <1 day. This is suggestive of an increase in the strength of convection. We find no significant positive trend in sea surface temperatures for this region in the HadISST1 data set using the online KNMI Climate Explorer. In two subtropical regions there is an increase in the number of events lasting 1–5 days, suggestive of increases in storminess. We find consistent increases in eddy-kinetic-energy for these regions in the ERA-Interim data set.

The total number of events between 40°S and 40°N that last between 1–2 days has significantly increased since 1980, consistent with the increased frequency of mesoscale organized deep convection found by *Tan et al.* [2015]. A simultaneous decrease in precipitation per event results in a smaller increase in 1–2 day event precipitation than would be expected from event density alone. The number of 2–5 day events was relatively stable until ~2000, and has seen a sharp increase since then. Whether these changes are an artifact of the ever evolving satellite data sets, or are representative of changes that have occurred in the character of precipitation over the past decades, is yet to be firmly established. That there is a positive trend in 1–2 day event frequency in both the TRMM and ERA-Interim data sets suggests the trend is real; however, these two data sets are based on some of the same satellite data. The result is robust to changing the minimum precipitation threshold, and there is no such trend in the smallest, or shortest-lived events, which might have indicated that increasing spatial resolution of observations was playing a significant role. Within the TRMM 3B42 data set the number of data points based on microwave precipitation estimates instead of infrared estimates increases strongly from 1998 to 2003, with little change thereafter. This timing is inconsistent with the observed trend in the number of events, suggesting that the shift from infrared to microwave estimates is not responsible for the trend in precipitation events.

If the trend in 1–5 day events is indeed real, examination of the spatial structure may present clues of possible mechanisms. The strongest positive regressions are seen in the tropical Pacific; this may be related to trends in Pacific trade winds observed by *England et al.* [2014]. Similarly, *Kim and Ha* [2015] show that there has been a pattern of precipitation in the tropical Pacific that has seen a strong positive regression since 1990, driven by global warming and natural decadal variability. We note that the Pacific Decadal Oscillation (PDO) index has generally been decreasing since the mid-1980s.

Event data sets for the TRMM 3B42 and ERA-Interim data have been made freely available online and can be used to further explore the character of precipitation events. Potential future studies include partitioning

events by, for example, total event precipitation or spatial footprint; or studying the evolution of event spatial footprint, or intensity, over event lifetimes. We hope these data will provide a gateway to improving our understanding of global precipitation as an event-based phenomenon.

Acknowledgments
The authors would like to thank two anonymous reviewers for comments that helped improve this manuscript, as well as Robert Houze, Mike Wallace, and George Huffman for fruitful discussions and comments. R.H. White was supported by the Joint Institute for the Study of the Atmosphere and Ocean and the Atmospheric Sciences department, at the University of Washington. D.S.B. was supported by a grant from the Tamaki Foundation. The KNMI Climate Explorer was used to explore the time evolution and variability of observational data sets. The TRMM 3B42 data were provided by the NASA/Goddard Space Flight Center's Mesoscale Atmospheric Processes Laboratory, and PPS, which develop and compute the TRMM 3B42 as a contribution to TRMM and archived at the NASA GES DISC; data set accessed on 5 October 2015. Interpolated OLR data were provided by the NOAA/OAR/ESRL PSD, Boulder, Colorado, USA, from their website at http://www.esrl.noaa.gov/psd/. The data sets and analysis code used in this work can be accessed from http://atmos.washington.edu/~rachel/precipevents.html.

References

Adler, R. F., G. J. Huffman, D. T. Bolvin, S. Curtis, and E. J. Nelkin (2000), Tropical rainfall distributions determined using TRMM combined with other satellite and rain gauge information, *J. Appl. Meteorol.*, *39*(12), 2007–2023, doi:10.1175/1520-0450(2001)040<2007:TRDDUT>2.0.CO;2.

Allan, R. P., B. J. Soden, V. O. John, W. Ingram, and P. Good (2010), Current changes in tropical precipitation, *Environ. Res. Lett.*, *5*(2), 25205.

Bates, B. C., Z. W. Kundzewicz, A. Wu, and J. P. Palutikof (2008), *Climate Change and Water*, 210 pp., Technical Paper of the Intergovernmental Panel on Clim. Change, IPCC Secretariat, Geneva, Switzerland.

Bauer, P., P. Lopez, D. Salmond, A. Benedetti, S. Saarinen, and M. Bonazzola (2006), Implementation of 1D+4D-Var assimilation of precipitation-affected microwave radiances at ECMWF. II: 4D-Var, *Q. J. R. Meteorol. Soc.*, *132*(620), 2307–2332, doi:10.1256/qj.06.07.

Berg, W., T. LâEcuyer, and J. M. Haynes (2009), The distribution of rainfall over oceans from spaceborne radars, *J. Appl. Meteorol. Climatol.*, *49*(3), 535–543, doi:10.1175/2009JAMC2330.1.

Berry, G., M. J. Reeder, and C. Jakob (2011), A global climatology of atmospheric fronts, *Geophys. Res. Lett.*, *38*, L04809, doi:10.1029/2010GL046451.

Catto, J. L., C. Jakob, G. Berry, and N. Nicholls (2012), Relating global precipitation to atmospheric fronts, *Geophys. Res. Lett.*, *39*, L10805, doi:10.1029/2012GL051736.

Chang, W., M. L. Stein, J. Wang, V. R. Kotamarthi, and E. J. Moyer (2016), Changes in spatiotemporal precipitation patterns in changing climate conditions, *J. Clim.*, *29*(23), 8355–8376, doi:10.1175/JCLI-D-15-0844.1.

Collins, M., et al. (2013), Long-term climate change: Projections, commitments and irreversibility, in *Climate Change 2013: The Physical Science Basis. Contribution of Working Group I to the Fifth Assessment Report of the Intergovernmental Panel on Climate Change*, edited by T. F. Stocker, pp. 1029–1136, Cambridge Univ. Press, Cambridge, U. K., and New York.

Dai, A. (2006), Precipitation characteristics in eighteen coupled climate models, *J. Clim.*, *19*(18), 4605–4630, doi:10.1175/JCLI3884.1.

Davis, C., B. Brown, and R. Bullock (2006), Object-based verification of precipitation forecasts. Part I: Methodology and application to mesoscale rain areas, *Mon. Weather Rev.*, *134*(7), 1772–1784, doi:10.1175/MWR3145.1.

Dee, D. P., et al. (2011), The ERA-Interim reanalysis: Configuration and performance of the data assimilation system, *Q. J. R. Meteorol. Soc.*, *137*(656), 553–597.

England, M. H., S. McGregor, P. Spence, G. A. Meehl, A. Timmermann, W. Cai, A. S. Gupta, M. J. McPhaden, A. Purich, and A. Santoso (2014), Recent intensification of wind-driven circulation in the Pacific and the ongoing warming hiatus, *Nat. Clim. Change*, *4*(3), 222–227, doi:10.1038/nclimate2106.

Gu, G., R. F. Adler, and G. J. Huffman (2016), Long-term changes/trends in surface temperature and precipitation during the satellite era (1979–2012), *Clim. Dyn.*, *46*(3–4), 1091–1105, doi:10.1007/s00382-015-2634-x.

Held, I. M., and B. J. Soden (2006), Robust responses of the hydrological cycle to global warming, *J. Clim.*, *19*(21), 5686–5699.

Houze, R. A., K. L. Rasmussen, M. D. Zuluaga, and S. R. Brodzik (2015), The variable nature of convection in the tropics and subtropics: A legacy of 16 years of the Tropical Rainfall Measuring Mission satellite, *Rev. Geophys.*, *53*, 994–1021, doi:10.1002/2015RG000488.

Huffman, G. J., and D. T. Bolvin (2014), TRMM and other data precipitation dataset documentation, TRMM Doc., Mesoscale Atmospheric Processes Laboratory, NASA Goddard Space Flight Center. [Available at https://pmm.nasa.gov/sites/default/files/document_files/3B42_3B43_doc_V7_4_19_17.pdf.]

Huffman, G. J., D. T. Bolvin, E. J. Nelkin, D. B. Wolff, R. F. Adler, G. Gu, Y. Hong, K. P. Bowman, and E. F. Stocker (2007), The TRMM Multisatellite Precipitation Analysis (TMPA): Quasi-global, multiyear, combined-sensor precipitation estimates at fine scales, *J. Hydrometeorol.*, *8*(1), 38–55, doi:10.1175/JHM560.1.

Kikuchi, K., and B. Wang (2008), Diurnal precipitation regimes in the global tropics, *J. Clim.*, *21*(11), 2680–2696, doi:10.1175/2007JCLI2051.1.

Kim, B.-H., and K.-J. Ha (2015), Observed changes of global and western Pacific precipitation associated with global warming SST mode and mega-ENSO SST mode, *Clim. Dyn.*, *45*(11–12), 3067–3075, doi:10.1007/s00382-015-2524-2.

Liebmann, B., and C. A. Smith (1996), Description of a complete (interpolated) outgoing longwave radiation dataset, *Bull. Am. Meteorol. Soc.*, *77*, 1275–1277.

Liu, C. (2010), Rainfall contributions from precipitation systems with different sizes, convective intensities, and durations over the tropics and subtropics, *J. Hydrometeorol.*, *12*(3), 394–412, doi:10.1175/2010JHM1320.1.

Liu, C., E. J. Zipser, D. J. Cecil, S. W. Nesbitt, and S. Sherwood (2008), A cloud and precipitation feature database from nine years of TRMM observations, *J. Appl. Meteorol. Climatol.*, *47*(10), 2712–2728, doi:10.1175/2008JAMC1890.1.

Nesbitt, S. W., and E. J. Zipser (2003), The diurnal cycle of rainfall and convective intensity according to three years of TRMM measurements, *J. Clim.*, *16*(10), 1456–1475, doi:10.1175/1520-0442(2003)016<1456:TDCORA>2.0.CO;2.

Nesbitt, S. W., E. J. Zipser, and D. J. Cecil (2000), A census of precipitation features in the tropics using TRMM: Radar, ice scattering, and lightning observations, *J. Clim.*, *13*(23), 4087–4106, doi:10.1175/1520-0442(2000)013<4087:ACOPFI>2.0.CO;2.

Simpson, J., C. Kummerow, W.-K. Tao, and R. F. Adler (1996), On the Tropical Rainfall Measuring Mission (TRMM), *Meteorol. Atmos. Phys.*, *60*(1–3), 19–36, doi:10.1007/BF01029783.

Skok, G., J. Tribbia, J. Rakovec, and B. Brown (2009), Object-based analysis of satellite-derived precipitation systems over the low- and midlatitude Pacific Ocean, *Mon. Weather Rev.*, *137*(10), 3196–3218, doi:10.1175/2009MWR2900.1.

Skok, G., J. Tribbia, and J. Rakovec (2010), Object-based analysis and verification of WRF model precipitation in the low- and midlatitude Pacific Ocean, *Mon. Weather Rev.*, *138*(12), 4561–4575, doi:10.1175/2010MWR3472.1.

Skok, G., J. Bacmeister, and J. Tribbia (2013), Analysis of tropical cyclone precipitation using an object-based algorithm, *J. Clim.*, *26*(8), 2563–2579, doi:10.1175/JCLI-D-12-00135.1.

Stephens, G. L., M. Z. Hakuba, M. Hawcroft, J. M. Haywood, A. Behrangi, J. E. Kay, and P. J. Webster (2016), The curious nature of the hemispheric symmetry of the Earth's water and energy balances, *Curr. Clim. Change Rep.*, *2*(4), 135–147, doi:10.1007/s40641-016-0043-9.

Tan, J., C. Jakob, W. B. Rossow, and G. Tselioudis (2015), Increases in tropical rainfall driven by changes in frequency of organized deep convection, *Nature*, *519*, 451–454, doi:10.1038/nature14339.

Trenberth, K. E., and G. R. Asrar (2014), Challenges and opportunities in water cycle research: WCRP contributions, *Surv. Geophys.*, *35*(3), 515–532, doi:10.1007/s10712-012-9214-y.

Trenberth, K. E., A. Dai, R. M. Rasmussen, and D. B. Parsons (2003), The changing character of precipitation, *Bull. Am. Meteorol. Soc.*, *84*(9), 1205–1217, doi:10.1175/BAMS-84-9-1205.

Venugopal, V., and J. M. Wallace (2016), Climatology of contribution-weighted tropical rain rates based on TRMM 3B42, *Geophys. Res. Lett.*, *43*, 10,439–10,447, doi:10.1002/2016GL069909.

Yang, S., and S. W. Nesbitt (2014), Statistical properties of precipitation as observed by the TRMM precipitation radar, *Geophys. Res. Lett.*, *41*, 5636–5643, doi:10.1002/2014GL060683.